Acta Astronautica 135 (2017) 192–197

Contents lists available at ScienceDirect

Acta Astronautica

journal homepage: www.elsevier.com/locate/aa

Advanced materials obtained by Spark Plasma Sintering

V.N. Chuvil'deev, M.S. Boldin *, A.V. Nokhrin, A.A. Popov

Lobachevsky State University of Nizhny Novgorod (National Research University), Research and Development Institute of Physics and Technology, 23 Prospect Gagarina (Gagarin Avenue), Nizhny Novgorod 603950, Russia

ARTICLE INFO

Article history:
Received 23 August 2016
Received in revised form
29 August 2016
Accepted 1 September 2016
Available online 4 September 2016

Keywords:
Spark Plasma Sintering
Ceramics
Alumina
Silicon carbide
Mechanical properties

ABSTRACT

This research paper provides an illustration of how to use the Spark Plasma Sintering technology (SPS) for powder materials in order to obtain lightweight ceramics (based on alumina) and describes physical principles ensuring efficiency of high heating rates for sintering high-temperature ceramics (pure silicon carbide). Optimization of SPS modes helps to produce Al_2O_3/ZrO_2 ceramics with grain size of less than 400 nm, microhardness H_v=24 GPa, and crack resistance K_{IC}=4.2 MPa $m^{1/2}$., and ceramics of pure SiC with grain size less than 50 nm, microhardness H_v=21 GPa and crack resistance coefficient K_{IC}=3.5 MPa $m^{1/2}$.

1. Introduction

Space vehicles being exposed to space environment are subjected to mechanical effects. The problem, connected with protection of orbital stations against ballistic exposure to "space debris", primarily to the components of the worked-out space vehicles, is widely discussed in scientific literature [1–6].

It should also be noted that rocket aerospace engineering is facing the problem of high thermal loading of structural elements, especially combustion chambers of rocket engines [7–9].

Currently, Spark Plasma Sintering (SPS) technology for high-speed compaction is widely used in powder material engineering. The SPS method has demonstrated its high efficiency in consolidating ceramics and metals nanomaterials, composites, solid materials, electronic materials, thermoelectric and biomaterials. The SPS method has several advantages that distinguish it from the traditional sintering methods such as hot pressing and sintering of precompacted billets without pressure. Specifically, SPS enables are liable control of the sintering process parameters and material microstructure [10].

2. High-temperature silicon carbide ceramics

Silicon Carbide (SiC) is one of the most advanced materials to produce engine components, nose cones, and other critical elements in aerospace engineering [11]. The reason for that lies in the fact that monocrystals of this material are characterized by high hardness ~ 27 GPa, low specific weight ~3.21 g/cm^3 and temperature stability up to T=2300 °C.

Traditional methods of producing SiC-based ceramics include loose sintering [12], reaction sintering [13] and hot pressing or pressure sintering [14–16]. These methods so far fail to sinter ceramics of pure SiC to a density close to a theoretical value.

To achieve higher density, the original SiC powder is supplemented with additives entering a liquid phase during sintering. Additives generally include MgO, Al_2O_3, Y_2O_3, AlN or their mixtures [13,15–18]. However, a low-melting component significantly limits an operating temperature range for such ceramics. Maximum operating temperatures of known SiC-based composites do not exceed 1500 °C.

Thus, a new technology of sintering pure silicon carbide (without additives) that would ensure high density and a homogeneous grain structure of ceramics becomes particularly relevant.

In the recent decade, high-speed compaction technology known as Spark Plasma Sintering (SPS) has become a frequent practice in powder engineering [19–21]. One of the features of SPS technology is an opportunity to obtain dense ceramics from carbide powders [22–26]. From this perspective, SPS method seems rather promising to obtain nanostructured high-density pure silicon carbide.

The research is carried out using nanodispersed (d~40–50 nm) powder β-SiC produced by "Alfa Aesar – A Johnson Matthey Company". To eliminate agglomerates, the original powder was subjected to ultrasonic treatment in distilled water (laced with surfactant Dispex A40) using a homogenizer HielscherUP200Ht.

* Corresponding author.
E-mail address: boldin@nifti.unn.ru (M.S. Boldin).

http://dx.doi.org/10.1016/j.actaastro.2016.09.002
0094-5765/

The resulting suspension was poured into a plaster mold with a Ø10 mm inner diameter and then placed in an oven at 70 °C for 24 h.

Compacting of a powdered blank with a Ø10 mm diameter was carried out using the spark plasma sintering technology (SPS) in a sintering unit "DR. SINTER model SPS-625 Spark Plasma Sintering System" (SPS SYNTEX INC. Ltd., Japan). The temperature was measured using a pyrometer centered on the outer surface of the graphite mold. The heating rate was 400°C/min, while the applied load remained under 70 MPa. Sintering took place in 6 Pa vacuum. Sintering took place at 2000 °C.

The density of sintered samples was measured using the hydrostatic weighing method in distilled water using Sartorius CPA scales. Accuracy of density calculations was ± 0.005 g/cm^3.

Vickers hardness (H_V) was measured using an automated microhardness tester "Struers Duramin-5" with a 2 kg load. Crack resistance K_{IC} was calculated using the Palmqvist method. Measuring accuracy of H_V and K_{IC} was ± 1.5 GPa and ± 0.5 MPa m$^{1/2}$ respectfully.

The microstructure of samples was studied with the help of a scanning electron microscope Jeol JSM-6490.

Fig. 1 shows dependence between sample density and holding time at T=2000°C. Microstructure of the SiC sample with 93% density is shown in Fig. 2. The grain size in resulting ceramics does not exceed the size of particles in the original powder. Microhardness of the sample obtained is H_v=21 GPa, crack resistance K_{IC}=3.5 MPa m$^{1/2}$.

Fig. 1 shows that high temperatures lead to reduced density of a sintered sample because of silicon carbide dissociation processes, thus the solution to the problem of obtaining high-density pure silicon carbide could not be found in the traditional approach that implies increasing the isothermal holding time.

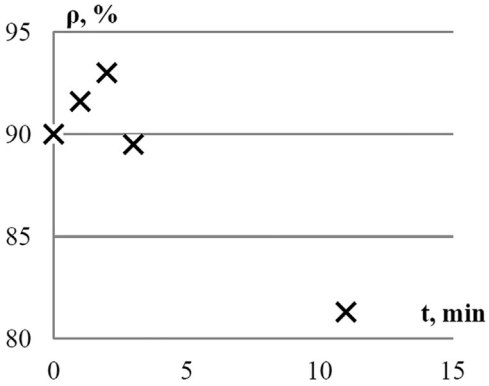

Fig. 1. Dependence between density and holding time.

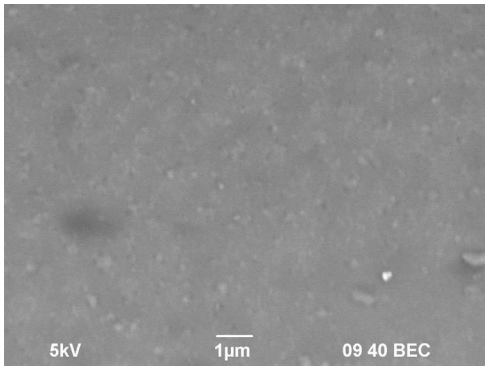

Fig. 2. Microstructure of a SiC sample (ρ=93%) obtained through SPS technology (SEM).

In order to choose the optimal SPS mode for SiC powder sintering, we shall consider shrinkage mechanisms. Normally, shrinkage intensity (I) or, in other words, intensity of mass transfer leading to the convergence of centers of contacting particles has a deformation component ($I(\dot{\varepsilon})$) and a diffusion component $\left(I\left(D_1^{eff}\cdot F^{eff}\right)\right)$:

$$I = I(\varepsilon') + I\left(D^{eff}\cdot F^{eff}\right) \quad (1)$$

where ε' – rate of plastic deformation under outer load, D_1^{eff} – effective diffusion coefficient, F^{eff} – effective driving force (F^{eff}).

Plastic deformation can be neglected during silicon carbide sintering, as this material is characterized by strong ionic-covalent bond of carbon and silicon atoms that explains high values of the dislocation glide activation energy. Our further study shall be limited to the analysis of the diffusion component expressed in the product of the effective diffusion coefficient and the effective driving force.

Effective diffusion coefficient in Eq. (1) is the sum of volume diffusion coefficient (D_V) and grain boundary diffusion coefficient (D_{GB}).

$$D^{eff} = D_V + \frac{\delta_{GB}}{d}D_{GB} \quad (2)$$

where δ_{GB} – diffusion thickness of grain boundaries, d – powder particle (grain) size.

When considering sintering processes, the main focus is usually on analyzing the intensity of diffusion flows, whereas the issue of how the driving force value is changing during sintering is given inadequate attention.

The equation for effective sintering force is as follows [27]:

$$F^{eff} = P^{eff} + \gamma\Delta \quad (3)$$

where P^{eff} – effective stress in the area of particle-to-particle contact caused by outer load, γ – surface energy, Δ – curvature of the contact area equal to the difference between the curvature of the particle surface and the curvature of the contact area surface ($\Delta = 1/a - 1/r$, where a – contact area radius, r – radius of sintered particles).

During SPS sintering the outer load is generally limited by the strength of graphite used as a material for a press mold and does not exceed 100 MPa (which corresponds to $\sim 6\cdot 10^{-4}$ G for silicon carbide) [28], but sintering acceleration usually occurs under pressure starting with 1 GPa ($\sim 10^{-3}$ G) [29]. Thus, in case of SPS, F^{eff} value is controlled mainly by $\gamma\Delta$ component. However, an estimate of the $\gamma\Delta$ for SiC particles of 1 μm in size equals $\sim 1.3\cdot 10^{-3}$ G.

It is crucial to highlight that Δ value is changing throughout the sintering process, as diffusion flows lead to a reduced curvature of the particle-to-particle contact area. The following equation is obtained to a first approximation:

$$\Delta \sim \left(D^{eff};\ \frac{\delta_S}{d}D_S;\ D_{vapor}\right)^{-n} \quad (4)$$

where δ_S – thickness of a layer where surface diffusion is emerging, D_s – surface diffusion coefficient, D_{vapor} – vapor diffusion coefficient, n – parameter depending on the nature of diffusion processes.

Curvature of the contact area Δ is changing most intensively in case of surface diffusion and vapor diffusion. These types of diffusion mass transfer start developing at low temperatures (see Fig. 3) and lead to changes in the form of sintered particles rather than convergence of their centers (contraction). This causes reduction in the driving force during sintering under slow heating. Fig. 3 shows activation energy values typical of most materials that